Mechanism-Based Inactivation of a Yeast Methylamine Oxidase Mutant: Implications for the Functional Role of the Consensus Sequence Surrounding Topaquinone†

Danying Cai,‡,§ Joanne Dove,‡ Nobuhumi Nakamura,‖ Joann Sanders-Loehr,‖ and Judith P. Klinman*,‡

Department of Chemistry, University of California, Berkeley, California 94720, and Department of Chemistry, Biochemistry and Molecular Biology, Oregon Graduate Institute of Science and Technology, Portland, Oregon 97291

Received April 8, 1997; Revised Manuscript Received July 7, 1997⊗

ABSTRACT: The copper-containing yeast methylamine oxidase E406N mutant has an altered consensus sequence surrounding the topaquinone cofactor (residue 405). The mutation has no effect on the final yield of the active-site topaquinone cofactor during biogenesis but causes the enzyme to be inactivated by substrate methylamine [Cai, D., and Klinman, J. P. (1994) *Biochemistry 33*, 7674−7653]. In this study we show that the inactivation leads to the formation of a covalent adduct, which has a UV/vis spectrum very similar to that of a product Schiff base, an intermediate of topaquinone-catalyzed amine oxidation reactions. The kinetic isotope effects on the second-order rate constant for the inactivation and catalytic turnover are identical, indicating that the two processes share a common intermediate that follows C–H bond cleavage. Resonance Raman spectroscopy provides direct evidence for the accumulation of a neutral product Schiff base species. Removal of excess methylamine leads to recovery of both activity and the native absorption spectrum for E406N, indicating that the cofactor in the inactivated enzyme is chemically competent for hydrolysis. The rate of the reactivation is slow, however; the shortest half-life of the inhibited E406N at 25 °C is 5.9 min at pH 6.15. pH effect experiments show that the inactivation and reactivation steps are controlled by a single ionizable group with a pK_a of 6.9−7.1; under basic conditions, when this residue is deprotonated, the inactivation is the fastest and the half-life of the inhibited enzyme is the longest. On the basis of the available crystal structures of copper amine oxidases, we propose that a histidine residue in the dimer interface is responsible for the observed ionization. In the wild-type enzyme this histidine is kept protonated by virtue of Glu at position 406. Unlike methylamine, the larger substrates ethylamine and benzylamine give normal turnover with E406N. Disruption of structure at the subunit interface in E406N may allow a rotation of the relatively small topa−product Schiff base complex (formed from methylamine) away from the active-site base to a conformation that is incompetent toward hydrolysis.

Polypeptide-linked 2,4,5-trihydroxyphenylalanine- (topa-) quinone is generated by oxidizing a tyrosyl residue in a posttranslational process (*1*). Topaquinone thus formed has been identified as the redox cofactor in a wide range of copper amine oxidases (*2*). Evidence has been amassed in support of a transamination mechanism for the catalysis. This entails the reaction of topaquinone with the primary amino group of the substrate amine to form the first intermediate, the substrate Schiff base. Abstraction of a proton from the α-carbon by an active-site base reduces the cofactor and forms the second intermediate called the product Schiff base. Hydrolysis of this intermediate releases the product aldehyde and generates the aminoquinol. Topaquinone is subsequently regenerated following the oxidation of reduced enzyme by dioxygen (*3*−*6*). The substrate and the product Schiff base species and the reduced cofactor have been characterized in topaquinone model compound-catalyzed amine oxidation reactions, where the formation of the substrate Schiff base is believed to be the rate-limiting step under anaerobic conditions (*5*, *6*). In the case of enzymatic catalysis, rapid scanning kinetic data suggest that the formation of the product Schiff base is the rate-limiting step in the reductive half-reaction (*7*), consistent with the ability to trap the substrate Schiff base using $NaCNBH_3$ as reductant (*8*, *9*). A mechanism involving common intermediates to the enzymatic reaction has been proposed for topaquinone-catalyzed amine oxidation in model compound systems (*5*, *6*, *10*).

Using a heterologous expression system and site-directed mutagenesis, we have shown that topaquinone formation in a yeast copper amine oxidase is dependent on an intact copper binding site (*11*, *12*), consistent with the original proposal of a self-processing mechanism in topaquinone biogenesis (*13*). A similar self-catalyzing process has been shown for several bacterial enzymes (*14*−*16*). Surprisingly, the consensus sequence (Asn-Tyr-Asp/Glu), which contains the precursor Tyr 405, was not found to be critical for cofactor production. Topaquinone was observed to be fully formed in the E406N mutant of the yeast methylamine oxidase. This indicates that the conserved negatively charged residue at the +1 position toward the C-terminus from topa

†Supported by grants from the NIH (GM39296 to J.P.K. and GM34468 to J.S.-L.).

* To whom correspondence should be addressed: Department of Chemistry and Molecular and Cell Biology, 239 Hildebrand Hall, University of California, Berkeley, CA 94720.

‡ University of California, Berkeley.

§ Current address: Affymax Research Institute, 3410 Central Expressway, Santa Clara, CA 95051.

‖ Oregon Graduate Institute of Science and Technology.

⊗ Abstract published in *Advance ACS Abstracts,* September 1, 1997.

S0006-2960(97)00812-X CCC: $14.00

does not play an essential role in the modification of the tyrosyl side chain (*12*). More recently, Tanizawa and coworkers have shown that replacement of Asp by Asn in the consensus sequence of the *Arthrobacter globiformis* amine oxidase leads to a somewhat reduced rate for cofactor production (*17*).

One very curious feature of the catalytic behavior of the yeast amine oxidase E406N mutant is its differential effect on catalytic turnover with various substrates: whereas ethylamine and benzylamine are turned over normally, the smallest substrate, methylamine, gives rise to rapid enzyme inactivation. This study presents a detailed investigation of the inactivation of the yeast methylamine oxidase E406N enzyme by methylamine. The inactivation appears to be mechanism-based. We present evidence that the inactivation is reversible, suggesting that the inhibited enzyme is arrested in a catalytically competent state. The kinetics of both the inactivation and reactivation have been studied as a function of pH, implicating a conserved histidine that interacts with E406 at the subunit interface. A structural model, based on the available X-ray structures for copper amine oxidases, is proposed to account for our observations.

MATERIALS AND METHODS

Materials. CH_3NH_2·HCl and CD_3NH_2·HCl were purchased from Aldrich and $^{14}CH_3NH_2$ from Amersham. The yeast methylamine oxidase E406N mutant protein was purified as described (*12*). The protein concentration was determined with a Bradford assay (*18*) using the Bio-Rad protein assay reagent; bovine serum albumin was the protein standard. The active-site quinone content was titrated with phenylhydrazine (*11*).

Inactivation of E406N. For batch inactivation, 5−10 μM E406N enzyme was prepared in 50 mM sodium pyrophosphate−phosphate buffer, pH 9.0, and a small volume of methylamine solution was added to a final concentration of 0.5 mM. The inactivation was monitored spectrophotometrically at room temperature using an HP 8452A spectrophotometer. The reaction was stopped by chilling after no further change in absorbance could be observed. The excess methylamine was removed at 4 °C by passing the solution through a DG-10 desalting column (Bio-Rad), which was preequilibrated with 5 mM sodium pyrophosphate, pH 9.0. To demonstrate the covalent attachment of methylamine to the inactivated enzyme and to determine the stoichiometry, the enzyme was incubated with ^{14}C-labeled methylamine for 25 min at room temperature and purified similarly at 4 °C.

Steady-State Kinetic Measurements. The rate of inactivation (v_{inact}) at each methylamine concentration was expressed as the ratio of the initial velocity of oxygen consumption (v_0) and the total oxygen consumed at the point of complete inactivation:

$$v_{inact} = \frac{\Delta[O_2]\ (\mu M/min)}{\text{total } [O_2] \text{ consumed } (\mu M)} \qquad (1)$$

The oxygen concentration in the solution was recorded using a Yellow Springs oxygen electrode (Yellow Springs Instrument). All reactions were carried out at 25 °C in an air-saturated buffer. Each measurement was initiated by the addition of an E406N solution to a final concentration of 0.092−0.13 μM active subunit for the kinetic isotope effect study or 0.17−0.28 μM for the pH study. The kinetic isotope effect was determined in sodium phosphate buffer, pH 7.7, with 0.017−0.35 mM CH_3NH_2 or 0.028−0.55 mM CD_3NH_2. Kinetic parameters for the inactivation (K_i and k_{inact}) and the catalysis (K_m and k_{cat}) were calculated by nonlinear regression fits to, respectively,

$$v_{inact} = \frac{k_{inact}[\text{methylamine}]}{K_i + [\text{methylamine}]} \qquad (2)$$

$$v_0 = \frac{k_{cat}[\text{enzyme subunit}][\text{methylamine}]}{K_m + [\text{methylamine}]} \qquad (3)$$

where the concentration of the enzyme subunit was the active quinone content determined by titration with phenylhydrazine (*11*). In the pH study, k_{inact} was determined at saturating methylamine concentrations (0.4−2.0 mM), and the buffers used either were 50 mM potassium phosphate or were prepared as described below for the reactivation studies.

Reactivation of Methylamine-Inhibited E406N. The inhibited enzyme, prepared in 5 mM sodium pyrophosphate, pH 9.0, as indicated above, was first warmed to the desired temperature. Concentrated buffer stocks were used to generate final buffer concentrations that were either 50 mM in sodium pyrophosphate or 5 mM sodium pyrophosphate and 45 mM potassium phosphate. A single sample of inactivated enzyme was first desalted in potassium phosphate, pH 7.2, to remove the pyrophosphate buffer and then assayed. The final ionic strength was 120 ± 20 mM, with the exception of the two highest pH values, where the ionic strength was 200 mM. No trend was observed in changing buffer composition or ionic strength within this range. The solution was then incubated and the spectrum was recorded over time. The pH of the solution thus prepared was measured again and recorded as the final value.

Preparation of Raman Samples. The inactivation was carried out in a capillary tube with 0.5 mM E406N in 50 mM sodium pyrophosphate, pH 9.0, and initiated with a small volume of CH_3NH_2 or CD_3NH_2 to a final concentration of 10 mM. Reactions were monitored optically until the absorbance change at 380 nm reached a maximum, at which point spectra were obtained. For reaction in D_2O, the enzyme was diluted 10-fold with 20 mM sodium phosphate buffer (pH reading 8.6) and reconcentrated by ultrafiltration in a Micron 30 (Amicon); inactivation was then initiated as above with CH_3NH_2.

Raman Spectroscopy. Spectra were obtained on a McPherson 2061 spectrograph (0.67 m, 1800-groove grating) using Kaiser Optical holographic supernotch filters and a Princeton Instruments (LN-1100PB) liquid N_2-cooled CCD detector. The excitation source was a Coherent Innova 302 Kr (413.1 nm) laser. Spectra were collected from samples in capillary tubes at 298 K using 413.1 nm excitation (20 mW), 90° scattering geometry, 6 cm^{-1} spectral resolution, and 5 min data accumulation. Peak frequencies were calibrated relative to an indene standard and are accurate to ±1 cm^{-1}. Spectra of samples substituted with isotopes were obtained under identical instrumental conditions such that frequency shifts are accurate to ±0.5 cm^{-1} (*19*).

RESULTS

Mechanism of Inactivation. The inactivation of E406N by the substrate methylamine was first observed as the

FIGURE 1: Oxygen consumption by E406N mutant enzyme. Five microliters of 100 mM methylamine was added to 985 μL of 50 mM sodium phosphate buffer, pH 7.7, and incubated in the oxygen electrode chamber at 25 °C for 10 min with stirring. The reaction was initiated by the addition of 10 μL of 1.5 mg/mL E406N enzyme solution, which contained 13 μM of the active subunit. The arrow indicates the point of the addition. The final concentration of the enzyme and methylamine were 0.13 μM active subunit and 500 μM, respectively.

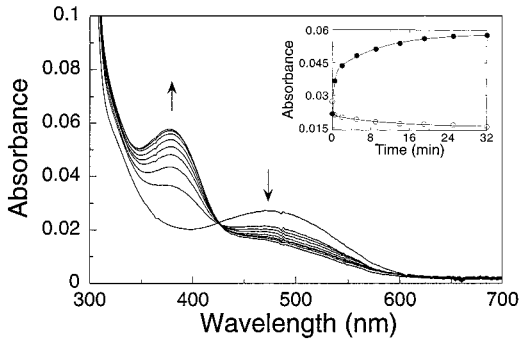

FIGURE 2: Spectral change during the incubation of E406N with methylamine. E406N enzyme (1.2 mg/mL) was prepared in 500 μL of 50 mM sodium pyrophosphate−phosphate buffer, pH 9.0. The solution was incubated at 20 °C and the spectrum recorded. Two microliters of 100 mM methylamine was then added and mixed immediately, and the spectrum was recorded 0.5, 2, 5, 9, 14, 17, 25, and 32 min after mixing. The arrows indicate the direction of the absorbance change, and the initial spectrum was without methylamine. (Inset) The absorbance changes at 380 (●) and 480 (○) nm over time are best fitted to double-exponential kinetics.

enzyme and methylamine were incubated under catalytic turnover conditions (Figure 1). The experiment showed that the oxidation of methylamine stopped after about 20 turnovers at neutral pH. Using substrates such as ethylamine or benzylamine with E406N, the rate of oxygen consumption would be linear within the same time period. This contrasts with the behavior of wild-type enzyme, which showed normal productive turnover with all substrates examined. The addition of excess methylamine to an E406N enzyme solution resulted in the disappearance of the absorbance at 472 nm and a concomitant appearance of a new peak at 376 nm (Figure 2). The absorbance change appears to be biphasic with an initial fast phase accounting for about half the total change, followed by a slow phase for the other half (Figure 2, inset). Preincubation of the enzyme with excess formaldehyde over the same period of time did not lead to any inhibition. We thus conclude that the inhibition by methylamine is caused by the direct interaction of the enzyme with methylamine and not by formaldehyde, the product from the methylamine oxidation.

The absorption at 472 nm is characteristic of the oxidized quinone cofactor in the active site of topaquinone-containing enzymes. Hence, a change in the spectrum indicates that the cofactor may be modified. To demonstrate covalent labeling, the enzyme was incubated with [^{14}C]-methylamine for 25 min. The reaction mixture was desalted to remove

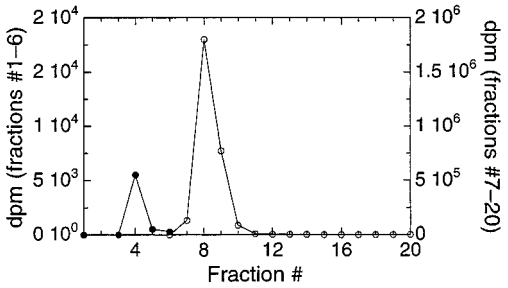

FIGURE 3: Radiolabeling of E406N protein. Protein (0.155 mg/mL, 1.3 μM active subunit) of an E406N enzyme sample in 50 mM sodium pyrophosphate−phosphate buffer, pH 9.0, was incubated at room temperature with 500 μM $^{14}CH_3NH_2$ (10 μCi/μmol). After 25 min, the mixture (200 μL) was desalted using a DG-10 column (10 mL), and the filtrate was collected in 1-mL fractions. The radioactivity and protein content in each fraction were determined and the total disintegrations per minute were plotted. The left axis is for fractions 1−6 (●), and the right axis is for fractions 7−20 (○). Only fraction 4 contained protein and its concentration was 0.029 mg/mL, which is equivalent to 0.245 μM active subunit.

excess methylamine from the protein and the radioactivity in all fractions was quantitated. The results showed that two radioactive peaks were eluted from the desalting column and that the first peak, which was contained in fraction 4, coincided with the protein (Figure 3). On the basis of the yield of protein (0.245 nmol of active subunits, representing 64% of the total protein concentration) and radioactivity (0.251 nmol), 100% of the protein that contained phenylhydrazine-titratable topaquinone was radiolabeled. This labeling supports the view that methylamine is forming a covalent bond with enzyme. Together with the UV/vis spectral data, we conclude that an adduct has formed between methylamine and the cofactor.

The chemical nature of the methylamine adduct has been determined by resonance Raman (RR) spectroscopy. The RR spectrum of E406N plus methylamine is dominated by a peak at 1622 cm^{-1} that shifts 59 cm^{-1} to lower energy with deuterated substrate (Figure 4A,C), thereby identifying it as the C═N stretch of a product imine (*20*). The 1622 cm^{-1} peak is unaffected by D_2O, indicating that no exchangeable protons are associated with this moiety, and the only spectral change in D_2O is the loss of the feature at 1299 cm^{-1} (Figure 4B). The RR spectrum of the unreacted yeast enzyme (data not shown) is completely different, with its major feature a ring mode at 1401 cm^{-1} and a weaker C═O stretch at 1678 cm^{-1}, as in other amine oxidases (*20*, *21*). Reactivation of the E406N mutant at pH 9.0 produced a RR spectrum that was superimposable with that of the unreacted enzyme.

Kinetics of Inactivation. k_{inact} was determined as a function of pH and the results showed that the inactivation was fastest at high pH. The dependence of k_{inact} on pH indicates a single ionizable group with a p$K_a = 6.9 \pm 0.2$ (Figure 5).

Kinetic isotope effects were determined for the methylamine oxidation and for the enzyme inactivation using CH_3NH_2 and CD_3NH_2 at pH 7.7. The results showed that, similar to the benzylamine oxidation by the wild-type yeast methylamine oxidase (*11*), there is an isotope effect on the k_{cat} and k_{cat}/K_m for the methylamine oxidation, indicating that C−H bond cleavage is partially rate-determining. There are also isotope effects on the k_{inact} and k_{inact}/K_i (Table 1). The size of the isotope effect for the inactivation $^D(k_{cat}/K_i)$ is very

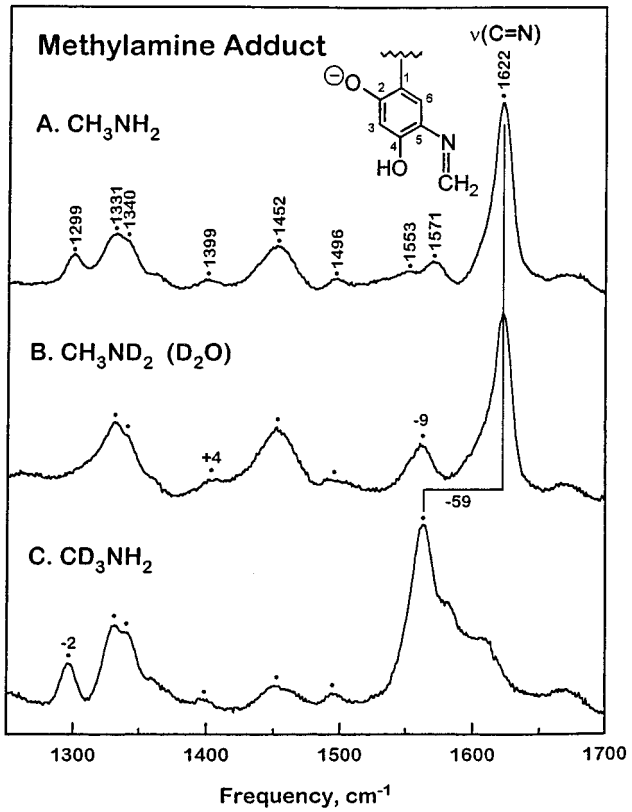

FIGURE 4: Resonance Raman spectra of E406N inactivated by methylamine: (A) CH_3NH_2, (B) CH_3ND_2 in D_2O, and (C) CD_3NH_2. Frequency shifts relative to spectrum A are listed above each peak; frequencies identical to spectrum A are unlabeled.

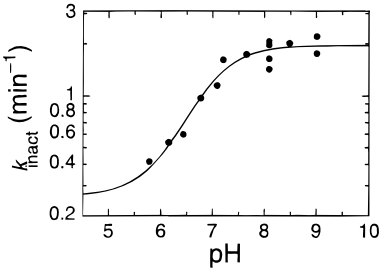

FIGURE 5: pH dependence of inactivation. The k_{inact} was measured at various pH values (see Materials and Methods). The line is the best nonlinear regression fit to the data with a pK_a = 6.9 ± 0.2, k_{inact} (fast) = 1.96 ± 0.09 min^{-1}, and k_{inact} (slow) = 0.26 ± 0.21 min^{-1}.

Table 1: Kinetic Isotope Effects on Inactivation and Catalysis[a]

	E406N		wild-type[c]
	inactivation	catalysis[b]	catalysis
k_{inact} or k_{cat} (s^{-1})	0.031 ± 0.002	0.769 ± 0.026	4.71
k_{inact}/K_i or k_{cat}/K_m (M^{-1} s^{-1})	(8.0 ± 2.1) × 10^2	(1.65 ± 0.19) × 10^4	3.2 × 10^4
$D_{(k)}$	1.20 ± 0.11	1.62 ± 0.11	ND[d]
$D_{(k/K)}$	2.38 ± 0.81	2.37 ± 0.58	ND

[a] Determined at 25 °C in 50 mM potassium phosphate, pH 7.7. [b] k_{cat} calculated on the basis of the subunit concentration. [c] Determined at 25 °C in 50 mM potassium phosphate, pH 7.2. Data taken from Cai and Klinman (*11*). [d] Not determined.

close to $^D(k_{cat}/K_m)$ for the catalysis while $^D(k_{inact})$ is somewhat smaller than $^D(k_{cat})$.

Stability of the Inactivated E406N and Kinetics of Reactivation. The removal of excess methylamine caused little immediate change in the spectrum of the inhibited enzyme (Figure 6A). However, over time, the absorption spectrum

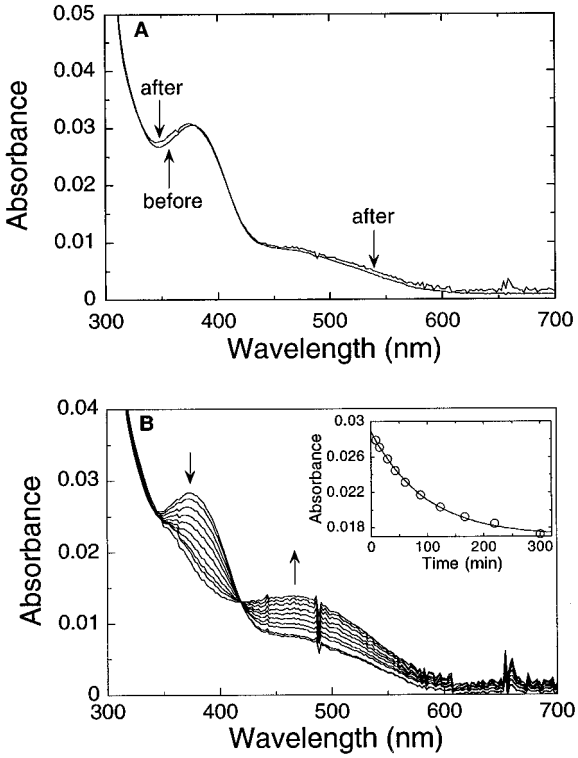

FIGURE 6: Stability of the inactivated E406N. (A) Spectra of the inactivated sample (from Figure 2) before and after desalting in 50 mM sodium pyrophosphate−phosphate buffer, pH 9.0. The scale of the spectrum was adjusted to account for the dilution after desalting. (B) Spectral change of the desalted sample over time. The desalted, methylamine-inactivated E406N was incubated in the desalting buffer and its spectrum was taken at 9, 15, 29, 43, 61, 88, 123, 166, 219, and 300 min after incubation. The arrows indicate the direction of the absorbance change. (Inset) Absorbance change at 380 nm fitted to single-exponential kinetics.

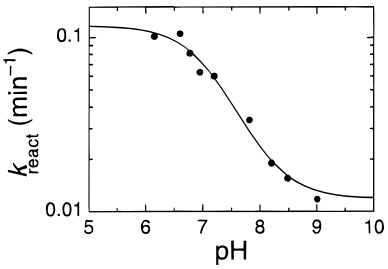

FIGURE 7: pH dependence of reactivation. The rate of the reactivation of the methylamine-inactivated E406N was measured at various pH (see Materials and Methods). The data were best fitted to a slow and a fast rate at high and low pH, respectively. The line is drawn with the following parameters: pK_a = 7.1 ± 0.2, k_{react} (fast) = 0.12 ± 0.01 min^{-1}, and k_{react} (slow) = 0.012 ± 0.005 min^{-1}.

of the enzyme was reverted back to one that was indistinguishable from the starting enzyme sample (Figure 6B). The spectral change appears to be first-order (Figure 6B, inset) and has an isosbestic point at 418 nm. Consistent with this observation, the ^{14}C-labeled E406N following desalting was found to gradually lose the radiolabel and the enzyme activity was regained.

The reactivation kinetics of the inhibited enzyme were affected by pH and temperature. The single-exponential rate constants were determined as a function of pH, and the results show that different from the inactivation, the reactivation occurs fastest under the acidic condition (Figure 7). The ionizable group controlling this process has a pK_a of 7.1 ±

0.2 and the half-lives of the inhibited enzyme at 25 °C were 5.9 min at pH 6.15 and 58 min at pH 9.01. Within the experimental error, this pK_a value is the same as that determined for the inactivation process.

No isotope effect was observed on the reactivation step, since the CD_3NH_2-inhibited enzyme had the same half-life as the CH_3NH_2-inhibited enzyme. Temperature increase can accelerate the reactivation process, which has an activation energy of 14 kcal/mol at neutral pH. On the basis of these observations, the inactivated E406N protein was always kept at 4 °C in pH 9 buffer to prolong its lifetime.

DISCUSSION

Studies with copper amine oxidases and topaquinone model compounds have provided very good evidence for an aminotransferase mechanism in topaquinone-catalyzed amine oxidation (*22*). The proposed reaction intermediates have been prepared and characterized in the model system (*6*). The formation of a substrate Schiff base in the enzymatic reaction was implicated in rapid scanning/stopped-flow experiments (*7*). The product Schiff base, however, could not be observed with the enzyme due to the apparently rapid rate of its hydrolysis.

The absorption peak at 372 nm for the methylamine-inhibited form of E406N has an estimated extinction coefficient of >6000 M^{-1} cm^{-1}. Because the λ_{max} is similar to that of a product Schiff base formed from a model compound and the ϵ value is significantly higher than that for a substrate Schiff base [ca. 1300 M^{-1} cm^{-1} at 352 nm in acetonitrile (*6*)], the cofactor in the methylamine-inhibited E406N is most likely trapped as a product Schiff base species. Substrate isotope effects (Table 1) support this view, since identical isotope effects have been observed for k_{cat}/K_m and k_{inact}/K_i, indicating that catalysis and inactivation share a common intermediate that occurs *after* the C–H bond cleavage step.

Confirmation of the structure of the inhibited enzyme comes from resonance Raman spectroscopy, Figure 4. The intense peak at 1622 cm^{-1} has been assigned to the C═N stretch of the imine on the basis of a −20 cm^{-1} isotopic shift when bovine serum amine oxidase was incubated anaerobically with ^{15}N-methylamine (*20*). Inactivation of E406N with the deuterated substrate should cause a shift in the frequency of the C═N stretch, which would allow differentiation between the substrate and product imines. Using the two mass system to calculate expected isotopic shifts with deuterated methylamine, the expected shift for the substrate and product imines would be −22 and −52 cm^{-1}, respectively (*20*). The observed isotopic shift of −59 cm^{-1} supports the product imine structure. From the absence of an effect of D_2O on the 1622 cm^{-1} peak, it appears that the imine is unprotonated.[1] A similar peak at 1301 cm^{-1} was observed in the methylamine adduct of phenethylamine oxidase generated under anaerobic conditions (*21*) and was assigned to the C–O stretch at the C-2 position on the basis of a −4 cm^{-1} shift with ^{18}O incorporated at the C-2 position during biogenesis. The frequency of this stretching mode is close to the range expected for a phenol and suggests that the cofactor is in the reduced state (*21*). The observed change in the 1299 cm^{-1} peak in D_2O further supports a reduced cofactor structure with a geometry that allows exchange of the C-2 hydroxyl with solvent.

Scheme 1: Proposed Inactivation Mechanism[a]

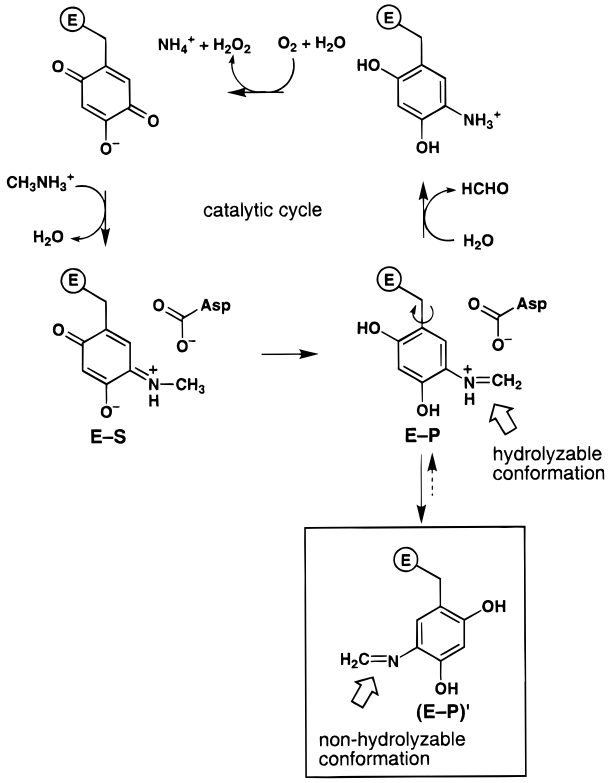

[a] The boxed intermediate (E−P)′ is the stable species detected.

Consistently, we have observed that the intermediate formed with E406N is chemically competent for hydrolysis to regenerate topaquinone. The major difference between the cofactor trapped in the inhibited E406N and the product Schiff base in the enzyme undergoing active catalytic turnover is that the rate of hydrolysis is very slow in the former. In order to account for the fact that the product Schiff base from methylamine in the inhibited E406N is catalytically competent yet kinetically stable, we propose that the structure of the inhibited enzyme prevents hydrolysis of the product Schiff base by water. Since the product Schiff base is readily cleaved by water under productive turnovers, a conformational change in either protein or cofactor is the simplest explanation for the observed inhibition. An important feature of the inhibition of E406N is its dependence on substrate size, with normal turnover occurring in the case of ethylamine and benzylamine. Rotation by 180° of a precursor to topaquinone in the course of its biogenesis has been postulated (*13*). It is possible that the small size of the product Schiff base from methylamine allows a rotation in E406N that places the reactive bond of this intermediate away from the active-site base required for facile attack by water (E–P′, Scheme 1). The postulated rotation under methylamine turnover may not occur when bulkier amines are used or when the wild-type enzyme is catalyzing the reaction. Hydrolysis and enzyme turnover can only occur to the product Schiff base in the initial conformation, E–P.

The pH effect studies on the inactivation and reactivation provide insight into how the protein controls these processes. We have observed an ionizable residue in the protein with a

[1] We can rule out a nonexchanging protium, since the entire reaction was carried out in D_2O. During the catalytic cycle, mechanistic studies have implicated the protonated form of both the substrate and product Schiff bases (*22*). Thus, a proton loss from the product Schiff base must occur along the inactivation path.

pK_a of 6.9−7.1. When this residue is deprotonated, the inactivation rate is 7.5 times that of the protonated form; additionally, the inactivated enzyme is 9.8 times more stable in its deprotonated than in its protonated form. It thus appears that deprotonation promotes the formation of a stable product Schiff base species by enhancing the rate of inactivation and slowing down the reactivation, with an overall factor of 74-fold. Possible candidates for the ionizing residue are the histidine at the dimer interface (see below) and the protonated product Schiff base. Ionization of the protonated Schiff base complex would be expected to reduce the rate of water attack and could increase the rate of the postulated ring flip:

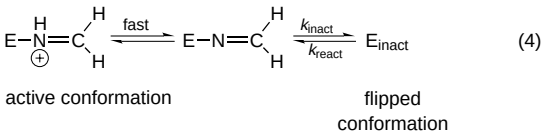

(4)

According to the mechanism in eq 4, only the ionized form of the Schiff base leads to inactive enzyme; in this instance, the pH dependence of k_{inact} reflects the pK_a of the product Schiff base. By microscopic reversibility, the flipping of the ring back to the active conformation would be expected to precede proton trapping, leading either to a pH-independent reactivation process or a process with a kinetically altered pK_a value. The identity of the observed pK_a for both inactivation and reactivation suggests instead the ionization of a residue that provides a pH-dependent "gating" for the postulated conformational change.[2] We propose this residue is the single histidine residue interacting with residue 406 at the dimer interface.

Four histidine residues are invariantly conserved in all known amine oxidase sequences (*23*, *24*). Three of them have been attributed to ligation of the active-site copper. This has been confirmed in the crystal structures of amine oxidases from *Escherichia coli* (*25*), pea seedling (*26*), and yeast (R. Li, J. P. Klinman, and F. S. Mathews, manuscript in preparation). The fourth histidine in the sequence of *E. coli* and pea seedling enzymes is found to form a hydrogen-bonding triad with a threonine and an aspartate. The Thr and Asp are two highly conserved residues contained within the active-site consensus sequence of amine oxidases (*23*, *24*). Although the corresponding residue for Asp in the yeast enzyme is a glutamate (E406), X-ray crystallographic studies indicate a similar overall fold and functional role for residues E406, T401, and H376 (R. Li, J. P. Klinman, and F. S. Mathews, manuscript in preparation). Due to electrostatic interactions between H376 and E406, one might expect that the His residue in the wild-type structure would have an elevated pK_a, such that it would remain protonated throughout the experimental pH range. Loss of this electrostatic interaction in the E406N mutant is proposed to disrupt the hydrogen-bonding network, reverting its pK_a to a normal range. The question is how, from a structural perspective, this change leads to inactivation of E406N by methylamine. Examination of the crystal structures for amine oxidases indicates that the conserved Asn at the +1 position toward the N terminus from topa sits in front of the mature cofactor and above the hydrogen-bonding triad (*25*, *26*) (R. Li, J. P. Klinman, and F. S. Mathews, (manuscript in preparation). Disruption of the triad stability, through deprotonation of His, may dislodge the Asn, creating a cavity for the postulated rotation of the topa−product Schiff base complex. This proposal also provides a possible functional role for the conserved residues that surround topa and are at the dimer interface in wild-type enzyme, via their participation in the orientation of the Tyr ring during its biogenesis to topaquinone.

One question that remains unanswered is why methylamine turns over normally with wild-type yeast methylamine oxidase while forming stable product Schiff base complexes with bovine serum amine oxidase and the phenethylamine oxidase from *Arthrobacter globiformis* (*cf. 20*). We note that the latter two enzymes, which preferentially oxidize large substrates such as benzylamine and phenethylamine, contain Asp at the position analogous to E406 in yeast methylamine oxidase. The smaller side chain at the +1 position toward the C terminus from topa in bovine serum amine oxidase and phenethylamine oxidase may preclude a catalytically viable cofactor configuration during turnover of very small substrates such as methylamine.

In contrast to model studies (*6*), the product Schiff base had never been directly observed in a topa-dependent enzyme turnover reaction. The data presented herein provide the first proof for the existence of a product Schiff base complex that is capable of entering the productive catalytic cycle.

[2] In light of the observation that the product Schiff base in inhibited enzyme is deprotonated, a mechanism must exist for proton loss. It is possible that ring flipping occurs with the protonated Schiff base that is subsequently deprotonated by an adjacent residue [e.g., a hydroxyl ion liganded to the active-site Cu(II)]. Alternatively, proton transfer from the product imine to the active-site base may precede ring flipping. Since pK_a perturbations appear to play a prominent role in enzyme-catalyzed, topaquinone-dependent reactions (*22*), loss of a proton from the protonated product Schiff base may be a natural consequence of the rotation of this species away from its likely counterion, the active-site base aspartate.

REFERENCES

1. Klinman, J. P., and Mu, D. (1994) *Annu. Rev. Biochem. 63*, 299−344.
2. McIntire, W. S., and Hartmann, C. (1993) in *Principles and Applications of Quinoproteins*: (Davidson, V. L., Ed.) pp 97−171, Marcel Dekker, Inc., New York.
3. Farnum, M., Palcic, M., and Klinman, J. P. (1986) *Biochemistry 25*, 1898−1904.
4. Janes, S. M., and Klinman, J. P. (1991) *Biochemistry 30*, 4599−4605.
5. Mure, M., and Klinman, J. P. (1995) *J. Am. Chem. Soc. 117*, 8698−8706.
6. Mure, M., and Klinman, J. P. (1995) *J. Am. Chem. Soc. 117*, 8707−8718.
7. Hartmann C., Brzovic P., and Klinman, J. P. (1993) *Biochemistry 32*, 2234−2241.
8. Hartmann, C., and Klinman, J. P. (1987) *J. Biol. Chem. 262*, 962−965.
9. Hartmann, C., and Klinman, J. P. (1990) *FEBS Lett. 261*, 441−444.
10. Wang, F. J., Bae, J. Y., Jacobson, A. R., Lee, L. M., and Sayre, L. M. (1994) *J. Org. Chem. 59*, 2409−2417.
11. Cai, D., and Klinman, J. P. (1994) *Biochemistry 33*, 7674−7653.
12. Cai, D., and Klinman, J. P. (1994) *J. Biol. Chem. 269*, 32039−32042.
13. Mu, D., Janes, S. M., Smith, A. J., Brown, D. E., Dooley, D. M., and Klinman, J. P. (1992) *J. Biol. Chem. 267*, 7979−7982.
14. Matsuzaki, R., Fukui, T., Sato, H., Ozaki, Y., and Tanizawa, K. (1994) *FEBS Lett. 351*, 360−364.

15. Matsuzaki, R., Suzuki, S., Yamaguchi, K., Fukui, T., and Tanizawa, K. (1995) *Biochemistry 34*, 4524−4530.
16. Choi, Y.-H., Matsuzaki, R., Fukui, T., Shimizu, E., Yorifuji, T., Sato, H., Ozaki, Y., and Tanizawa, K. (1995) *J. Biol. Chem. 270*, 4712−4720.
17. Choi, Y.-H., Matsuzaki, R., Suzuki, S., and Tanizawa, K. (1996) *J. Biol. Chem. 271*, 22598−22603.
18. Bradford, M. (1976) *Anal. Biochem. 72*, 248−254.
19. Loehr, T. M., and Sanders-Loehr, J. (1993) *Methods Enzymol. 226*, 431−470.
20. Nakamura, N., Moënne-Loccoz, P., Tanizawa, K., Suzuki, S., Mure, M., Klinman, J. P., and Sanders-Loehr, J. (1997) *Biochemistry 36*, 11479−11486.
21. Nakamura, N., Matsuzaki, R., Chio, Y.-H., Tanizawa, K., and Sanders-Loehr, J. (1996) *J. Biol.Chem. 271*, 4718−4724.
22. Klinman, J. P. (1996) *Chem. Rev. 96*, 2541−2561.
23. Mu, D., Medzihradszky, K. F., Adams, G. W., Mayer, P., Hines, W. M., Burlingame, A. L., Smith, A. J., Cai, D., and Klinman, J. P. (1994) *J. Biol. Chem. 269*, 9926−9932.
24. Tipping, A. J., and McPherson, M. J. (1995) *J. Biol. Chem. 270*, 16939−16946.
25. Parsons, M. R., Convery, M. A., Wilmot, C. M., Yadav, K. D. S., Blakeley, V., Corner, A. S., Philips, S. E. V., McPherson, M. J., and Knowles, P. F. (1995) *Structure 3*, 1171−1184.
26. Kumar, V., Dooley, D. M., Freeman, H. C., Guss, J. M., Harvey, I., McGuirl, M. A., Wilce, M. C. J., and Zubak, V. M. (1996) *Structure 4*, 943−955.

BI970812G